

Organ-based tube current modulation in chest CT. A comparison of three vendors

B.R. Mussmann^{a, b, c, *}, S.D. Mørup^d, P.M. Skov^a, S. Foley^e, A.S. Brenøe^a, F. Eldahl^a, G.M. Jørgensen^a, H. Precht^{d, f}

^a Department of Radiology, Odense University Hospital, Denmark

^b Department of Clinical Research, University of Southern Denmark

^c Faculty of Health Sciences, Oslo Metropolitan University, Norway

^d Conrad Research Programme, Centre for Applied Welfare Research, University College Lillebaelt, Denmark

^e Radiography & Diagnostic Imaging, School of Medicine, University College Dublin, Ireland

^f Medical Research Department, Odense University Hospital, Svendborg, Denmark

ARTICLE INFO

Article history:

Received 22 October 2019

Received in revised form

20 April 2020

Accepted 21 April 2020

Available online 10 May 2020

Keywords:

Chest

Computed tomography

Radiation dose

Image quality

ABSTRACT

Introduction: Organ-based tube current modulation (OBTCM) is designed for anterior dose reduction in Computed Tomography (CT). The purpose was to assess dose reduction capability in chest CT using three organ dose modulation systems at different kVp settings. Furthermore, noise, diagnostic image quality and tumour detection was assessed.

Methods: A Lungman phantom was scanned with and without OBTCM at 80–135/140 kVp using three CT scanners; Canon Aquillion Prime, GE Revolution CT and Siemens Somatom Flash. Thermo-luminescent dosimeters were attached to the phantom surface and all scans were repeated five times. Image noise was measured in three ROIs at the level of the carina. Three observers visually scored the images using a five-step scale. A Wilcoxon Signed-Rank test was used for statistical analysis of differences.

Results: Using the GE revolution CT scanner, dose reductions between 1.10 mSv (12%) and 1.56 mSv (24%) ($p < 0.01$) were found in the anterior segment and no differences posteriorly and laterally. Total dose reductions between 0.64 (8%) and 0.91 mSv (13%) were found across kVp levels ($p < 0.00001$). Maximum noise increase with OBTCM was 0.8 HU. With the Canon system, anterior dose reductions of 6–10% and total dose reduction of 0.74–0.76 mSv across kVp levels ($p < 0.001$) were found with a maximum noise increase of 1.1 HU. For the Siemens system, dose increased by 22–51% anteriorly; except at 100 kVp where no dose difference was found. Noise decreased by 1 to 1.5 HU.

Conclusion: Organ based tube current modulation is capable of anterior and total dose reduction with minimal loss of image quality in vendors that do not increase posterior dose.

Implications for practice: This research highlights the importance of being familiar with dose reduction technologies.

© 2020 The College of Radiographers. Published by Elsevier Ltd. All rights reserved.

Introduction

Organ-based tube current modulation (OBTCM) is a technique designed for anterior dose reduction, potentially reducing radiation

dose to radiosensitive organs such as the breasts and eye lens in computed tomography (CT). The major vendors have specific solutions, and all systems decrease the tube current when the tube is within a specified angle between 120 and 180° anteriorly.^{1–3} Resulting dose reduction of up to 50% to the breasts and other anterior organs has been demonstrated^{2,4,5} with acceptable noise increase up to 16%.^{6–8} While the Siemens OBTCM system increase tube current posteriorly to maintain image quality, the GE and Canon systems similarly reduce tube current anteriorly, but do not increase posteriorly and thus, image quality may be affected. Bismuth shielding may reduce dose similarly, but it has disadvantages,

* Corresponding author. Department of Radiology, Odense University Hospital, Denmark.

E-mail addresses: Bo.mussmann@rsyd.dk (B.R. Mussmann), sdmo@ucl.dk (S.D. Mørup), Peter.Skov-Madsen@rsyd.dk (P.M. Skov), anne-sofie.brenoee@rsyd.dk (A.S. Brenøe), Frank.Eldahl@rsyd.dk (F. Eldahl), Gitte.Maria.Jorgensen@rsyd.dk (G.M. Jørgensen), hepr@ucl.dk (H. Precht).

i.e. reduced signal and artefacts^{9,10} and especially the risk of increased dose when used in combination with automatic exposure control. Thus, the American Association of Physicists in Medicine recommends using other approaches to reduce the radiation dose to radiosensitive organs.¹¹ OBTCM is a more efficacious method with proven dose reduction potential in breast, head, neck and thyroid both experimentally and clinically.^{12–17} However, to our knowledge no studies have compared the dose reduction potential between kVp-levels and vendors.

This project set out to examine dose reduction in chest CT using different organ dose modulation systems at different kVp settings when diagnostic image quality, including the visibility of lung nodules was assessed.

Methods

In this experimental phantom study radiation dose and image quality in chest CT was compared across three CT scanners with and without organ dose modulation at a range of kVp settings.

According to Danish law ethical approval was not required for this research project as scans were performed on a phantom.

Phantom

An adult anthropomorphic N1 Lungman chest phantom (Kyoto Kagaku Co., Kyoto, Japan) was used with in-house custom-designed breasts containing a volume of 574 mL, reflecting the average breast size in a Caucasian sample.¹⁸ To determine the material used for the breast, Hounsfield unit (HU) measurements were performed in a sample of 50 female patients using PACS data, with a range between –23.0 and –98.0 HU, respectively, with a mean of –56.4. The breasts consisted of a mixture of refined porcine fat (1040 g), egg whites (310 g) and gelatin (36 g) with an attenuation of –56 HU at 120 kVp, simulating the attenuation of female breast tissue. Each breast was casted in a form that simulated the breast in a supine position and was subsequently attached to the phantom (Fig. 1).

Six phantom tumours were positioned in the chest cavity in different positions according to Table 1. The tumours covered the relevant sizes, types and risk categories in the Fleischner guidelines,¹⁹ i.e. with attenuation of 100 HU mimicking solid nodules and –630 HU mimicking subsolid nodules and diameters of 5, 8 and 12 mm. The exact position of each tumour was changed between

Table 1

Diameter and anatomical position of the phantom tumours. Attenuation was 100 and –630 HU for each tumour size.

Diameter (mm)	Anatomical position
5	Lung tissue: - Apical right/left - Lower lobe right/left
8	Subpleural
12	Hilus region, right/left

each scan and a scan without tumours was acquired at each kV step (Fig. 2.).

Image acquisition

The study was performed using three CT-scanners: Canon Aquilion Prime (Canon Medical Systems Corporation, Otawara Tochigi, Japan), GE Revolution CT (GE Healthcare, Waukesha, WI, USA) and Siemens Somatom Flash (Siemens Healthcare GmbH, Erlangen, Germany). All scans were performed using standard clinical chest protocols, with and without organ based tube current modulation. The technical settings for the scan protocols are listed in Table 2. The scanners were all calibrated according to department quality assurance protocols and the scans were repeated five times at each setting to allow averaging of dose measurements and to compensate for generator instability, tube fluctuations and variation in X-ray tube position during helical rotations.

Radiation dose measurements

Absorbed equivalent radiation dose was measured using MTS-N type 100 thermo-luminescent dosimeters (TLD) (Radcard s.c., Kraków, Poland) annealed and calibrated according to International Electrotechnical Commission report 1066, Feb. 1993 using an IR-2000 dosimeter irradiator (RadPro International GmbH, Wermelskirchen, Germany) containing a Strontium-90 source with a reference dose of 443 µSv. The TLDs were positioned at a single anatomical level corresponding to the centre of the breasts at eight different locations on the surface of the phantom (Fig. 2) and radiation dose was recorded using a RE-2000 automatic TLD reader (RadPro International GmbH, Wermelskirchen, Germany). According to the manufacturer the TLDs have a sensitivity spread of ±4.5%. Four TLDs were used to measure the background radiation. Displayed Dose length Product (DLP) was also recorded for each scan.

Image quality assessment

Image quality was assessed using visual grading analysis (VGA)²⁰ performed by three radiologists with 6, 14 and 22 years of experience using a five-point scale according to Ludewig et al.²¹ (Table 3). The images were presented using ViewDex^{22,23} and a 2MP monitor with a luminance of 170 cd/m² quality checked and maintained according to DICOM part 14, Grayscale Standard Display Function and. The images were presented as image stacks in random order scored according to predefined VGA image criteria, i.e. visually sharp reproduction of the trachea, main bronchi and the large and medium sized pulmonary vessels. Furthermore, the observers would assess the degree of detail of the pathology and approve or disapprove each image for diagnostic use. The criteria were validated by the radiologists prior to the VGA. The observers individually viewed images using fixed lung and mediastinum windows. Furthermore, they were blinded to exposure settings and to other observers' assessments. When the observers identified a



Figure 1. Image of the in-house custom-designed breasts attached to the phantom.

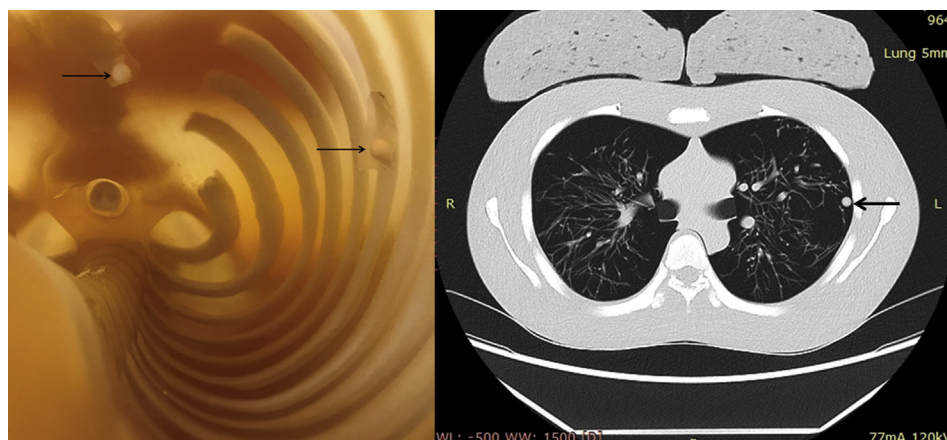


Figure 2. Left: Inside view of the Lungman phantom with two 8 mm tumours attached to the thoracic wall. Lung tissue was inserted after positioning of the tumours. Right: Corresponding 120 kVp 5 mm CT image (without OBTCM) with one of the subpleural tumours visible.

Table 2

Scan acquisition parameters for three scanners.

Scanner model	Canon Aquilion Prime	GE revolution	Siemens Somatom Flash
Tube voltage (kVp)	80, 100, 120, 135	80, 100, 120, 140	80, 100, 120, 140
Image quality metric	SD 10	Noise Index 27	Reference mAs 130
Reconstruction	AIDR 3D ^a	ASiR V ^b	SAFIRE 2 ^c
Scan range	315 mm	315 mm	315 mm
Pitch	0.813	0.992	1.2 (without OBTCM) 0.6 (with OBTCM)
Rotation time	0.35	0.5	0.5
Bowtie filter	Body	Body	Body
Detector configuration	80 × 0.5 mm	128 × 0.625	128 × 0.6
Modulation range	120°	180°	120°

^a Adaptive iterative dose reduction.

^b Adaptive statistical iterative reconstruction.

^c Sinogram affirmed iterative reconstruction.

Table 3

Visual grading analysis rating scale used by the observers.

Image score	Description
1	Poor image quality - image not useable, loss of information
2	Restricted image quality - Limited clinical value, clear loss of information
3	Sufficient image quality - Moderate limitations for clinical use, no substantial loss of information
4	Good image quality - Minimal limitations for clinical use,
5	Excellent image quality - No limitations for clinical use

tumour it was marked in a sketch image with an axial and a coronal drawing of the lungs. Furthermore, to test for intra-reader consistency, two duplicate images for each vendor were shown to observers.

Noise was measured by a single observer using standard deviation (SD) of Hounsfield values in three circular ROIs 12.5 mm in diameter positioned in the right pulmonary artery, vertebral body and in free air anterior to the phantom, respectively in one 5 mm slice at the level of the carina (Fig. 3).

Statistical analysis

Following normality testing using the Shapiro–Wilks test, continuous variables were summarized by descriptive statistics, i.e.

mean, standard deviation (SD) and number of observations or median and interquartile range (IQR) depending on data distribution. Radiation dose differences between scanners and between organ based modulation and no modulation were assessed using Wilcoxon Signed Rank test and noise measurements were assessed using the paired t-test. p-values ≤ 0.05 were considered statistically significant.

Differences between the observers' mean image quality scores (VGAS) were compared using Wilcoxon Signed Rank test. The degree of inter-observer agreement was determined using the Fleiss Kappa statistic, which is suitable when more than two observers are compared.²⁴

The detection of tumours between organ dose modulation systems were described as number of observations and proportions

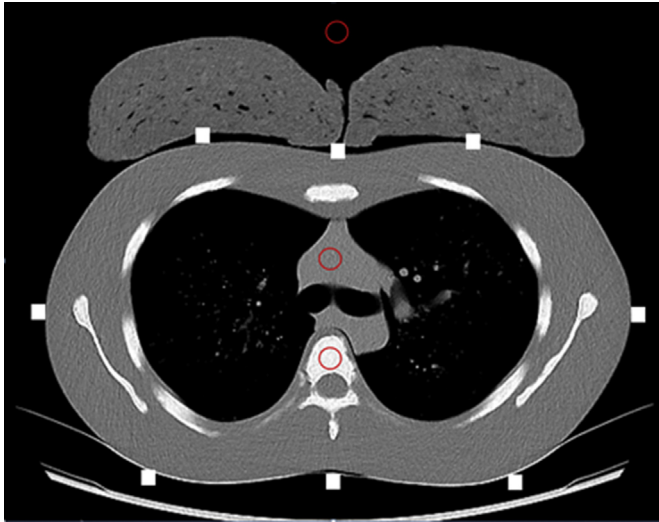


Figure 3. Circular Ø12.5 mm ROIs (red) positioned in the right pulmonary artery, vertebral body and in free air for noise measurements and TLDs (white boxes) positioned around the phantom. (For interpretation of the references to colour in this figure legend, the reader is referred to the Web version of this article.)

and analysis of intra-rater agreement was performed using Cohen's kappa.

All analyses were performed using STATA/IC 15.0 (StataCorp. LP, College Station, TX 77845 USA).

Results

A total of 120 scans were performed using the three different scanners at varying kVp levels, resulting in 480 TLD measurements.

Radiation dose

For the GE scanner, the mean absorbed doses, with and without OBTCM, at all kVp-levels are listed in Table 4a. There were no differences posteriorly and laterally while a statistically significant dose reduction between 12% at 140 kVp and 24% at 80 kVp was found in the anterior segment. In addition, a statistically significant total dose reduction was found at all kVp levels. The total dose reduction using OBTCM was 11, 13, 8 and 13% for 80 to 140 kVp, respectively, i.e. no obvious relationship between kVp-level and dose reduction was seen. A similar pattern was seen in the Canon

scanner with anterior dose reductions of 6–10% (Table 4b) and statistically significant total dose reduction at all kVp levels. In the Siemens scanner the anterior radiation dose increased up to 51% with OBTCM engaged and a total dose increase between 11% at 80 kVp and 32% at 120 kVp. The anterior and total dose increase was statistically significant at 80, 120 and 140 kVp (Table 4c).

Image quality

Noise measurements from all vendors are listed in Table 5. The maximum noise increase between OBTCM and non-OBTCM was found with the Canon CT scanner at 80 kVp where the average noise increased from 9.0 to 10.1 HU ($p = 0.003$).

The image quality was assessed by three observers in 12 scans per scanner ($n = 108$; no. of observations = 324). For the GE system, the VGAS across all kVp levels was 3.6 and 3.4 with and without OBTCM, respectively ($p = 0.27$), while for Canon we found equal VGAS of 3.6 ($p = 0.26$), while with Siemens the VGAS with and without OBTCM was 4.0 and 3.6, respectively ($p = 0.052$). The overall kappa value was 0.03 reflecting poor inter-observer agreement of the image quality scores between the three observers. The most experienced observer had 67% absolute agreement between first and second reading, kappa = 0.45 (i.e. weak agreement²⁵), while the two other radiologists had 33% and 42% agreement and kappa values of -0.3 and -0.1 (i.e. no agreement), respectively. However, in 81 of 108 images there were either complete agreement ($n = 17$) or the disagreement was 1 step on the scale ($n = 65$). In all cases across scanners and parameter settings the observers agreed that the images were suitable for diagnostic use.

Tumour visibility

All six images without tumours were correctly identified by all radiologists regardless of vendor, kVp and OBTCM settings. Without OBTCM the radiologists correctly identified 82, 86 and 92% of tumours, respectively and 85, 86 and 96% with OBTCM ($n = 72$). One false positive tumour was found in the right middle lobe by the radiologist with least experience. The rate of missed tumours with OBTCM versus non-OBTCM was: GE 6/10; Canon 8/4 and Siemens 10/15.

The total number of missed tumours was 24 with and 29 without OBTCM. The distribution of tumour size and attenuation is listed in Table 6.

Table 4a

Mean DLP, absorbed equivalent dose and standard deviation (SD) in mSv in different anatomical sites and various kVp levels. Vendor: GE.

Protocol	Mean DLP	Anterior n = 15	Posterior n = 15	Lateral, sin. n = 5	Lateral, dxt. n = 5	Average n = 40
80 kVp	90.94	6.51 (0.62)	6.20 (0.90)	5.64 (1.15)	6.20 (1.20)	6.25 (0.89)
80 kVp, OBTCM	79.04	4.95 (0.31)	6.14 (0.81)	5.03 (1.16)	6.08 (1.00)	5.55 (0.92)
Δ Dose, %	–	–24.0	–1.0	–10.8	–1.9	–11.2
p-value	–	<0.001	1.0000	0.89	0.89	0.004
100 kVp	110.37	6.85 (0.62)	7.07 (0.59)	6.96 (0.57)	6.77 (1.48)	6.94 (0.73)
100 kVp, OBTCM	97.17	5.72 (0.40)	6.42 (0.76)	5.96 (0.84)	5.85 (1.08)	6.03 (0.74)
Δ Dose, %	–	–16.5	–9.2	–14.4	–13.6	–13.1
p-value	–	0.0008	0.01	0.14	0.50	<0.00001
120 kVp	139.56	8.44 (0.54)	7.70 (0.82)	7.43 (1.77)	7.84 (1.09)	7.96 (0.97)
120 kVp, OBTCM	124.90	7.00 (0.48)	7.57 (0.99)	6.97 (1.25)	7.90 (0.76)	7.32 (0.88)
Δ Dose, %	–	–17.1	–1.7	–6.2	+0.7	–8.0
p-value	–	0.0008	0.82	0.50	0.89	0.009
140 kVp	169.36	9.44 (0.51)	9.45 (1.01)	8.14 (1.66)	9.27 (0.61)	9.26 (0.99)
140 kVp, OBTCM	156.50	8.34 (0.56)	8.92 (0.87)	6.79 (1.47)	7.64 (1.82)	8.28 (1.20)
Δ Dose, %	–	–11.7	–5.6	–16.6	–17.6	–10.6
p-value	–	0.0007	0.06	0.35	0.22	0.0001

Statistically significant ($p < 0.05$) results are marked in bold.

Table 4b

Mean absorbed equivalent dose and standard deviation (SD) in mSv in different anatomical sites and various kVp levels. Vendor: Canon.

Protocol	Mean DLP	Anterior n = 15	Posterior n = 15	Lateral, sin. n = 5	Lateral, dxt. n = 5	Average, n = 40
80 kVp	141.28	12.00 (1.86)	10.47 (1.21)	16.39 (1.28)	10.19 (1.15)	11.75 (2.41)
80 kVp, OBTCM	136.82	11.17 (1.64)	9.91 (1.04)	14.94 (1.37)	9.79 (1.01)	10.99 (2.07)
Δ Dose, %	–	–6.9	–0.05	–8.8	–3.9	–6.5
p-value	–	0.01	0.008	0.08	0.69	0.0002
100 kVp	124.62	11.26 (1.81)	9.81 (1.48)	15.63 (1.54)	8.07 (0.92)	10.86 (2.59)
100 kVp, OBTCM	126.30	10.56 (1.66)	9.84 (1.38)	14.27 (0.61)	7.29 (0.42)	10.34 (2.24)
Δ Dose, %	–	–6.2	+0.3	–8.7	–9.7	–4.8
p-value	–	0.009	0.73	0.14	0.22	0.009
120 kVp	148.08	12.38 (1.98)	11.75 (1.30)	14.49 (0.21)	9.68 (1.03)	12.07 (1.92)
120 kVp, OBTCM	141.32	11.58 (1.44)	11.16 (1.30)	14.68 (1.39)	9.00 (0.87)	11.49 (1.94)
Δ Dose, %	–	–6.5	–5.0	–1.3	–7.0	–4.8
p-value	–	0.01	0.21	0.89	0.22	0.006
135 kVp	181.20	16.13 (2.75)	15.16 (2.08)	18.97 (0.56)	12.09 (1.00)	15.61 (1.92)
135 kVp, OBTCM	172.72	14.49 (2.26)	15.14 (1.90)	17.65 (0.55)	12.43 (1.80)	14.87 (2.31)
Δ Dose, %	–	–10.2	–0.1	–7.0	–2.8	–4.7
p-value	–	0.004	0.95	0.04	0.89	0.006

Statistically significant ($p < 0.05$) results are marked in bold.**Table 4c**

Mean absorbed equivalent dose and standard deviation (SD) in mSv in different anatomical sites and various kVp levels. Vendor: Siemens.

Protocol	Mean DLP	Anterior n = 15	Posterior n = 15	Lateral, sin. n = 5	Lateral, dxt. n = 5	Average n = 40
80 kVp	231.50	10.68 (0.98)	10.88 (1.22)	9.67 (1.54)	10.62 (1.61)	10.62 (1.24)
80 kVp, OBTCM	239.50	16.13 (3.90)	18.26 (4.36)	17.90 (2.88)	15.92 (1.68)	17.12 (3.83)
Δ Dose, %	–	+51.0	+67.8	+85.1	+49.9	+61.2
p-value	–	0.0007	0.0007	0.04	0.04	<0.00001
100 kVp	238.28	12.48 (1.11)	13.62 (1.95)	14.31 (3.03)	12.92 (3.21)	13.19 (2.06)
100 kVp, OBTCM	220.86	13.41 (3.45)	14.27 (3.51)	14.58 (1.74)	13.03 (1.30)	13.83 (3.08)
Δ Dose, %	–	+7.5	+4.8	+1.9	+0.1	+0.6
p-value	–	0.39	0.61	0.89	0.89	0.41
120 kVp	261.7	13.65 (2.05)	13.16 (1.43)	12.93 (4.31)	13.66 (4.01)	13.38 (2.42)
120 kVp, OBTCM	258.72	17.46 (4.41)	17.78 (3.79)	17.95 (3.14)	17.35 (1.89)	17.63 (3.68)
Δ Dose, %	–	+27.9	+35.1	+38.8	+27.0	+31.8
p-value	–	0.009	0.002	0.04	0.14	<0.0001
140 kVp	300.56	15.83 (1.85)	15.86 (1.63)	16.98 (3.99)	15.49 (4.31)	15.94 (2.43)
140 kVp, OBTCM	306.68	19.36 (4.46)	20.67 (5.00)	19.64 (1.59)	17.65 (1.78)	19.67 (4.61)
Δ Dose, %	–	+22.3	+30.3	+15.7	+13.9	+23.4
p-value	–	0.004	0.005	0.22	0.50	0.0001

Statistically significant ($p < 0.05$) results are marked in bold.**Table 5**

Mean noise, SD and range in Hounsfield Units between kVp levels and scanners. Number of observations pr. scanner = 120 (i.e. three ROI measures pr. slice).

GE	CANON		Siemens	
	Noise	Range	Noise	Range
80 kVp	9.5 (2.1)	6.9–12.8	9.0 (1.7)	5.8–11.4
OBTCM	10.3 (2.1)	7.6–13.8	10.1 (1.7)	7.7–12.6
Difference	0.8	–	1.1	–
p-value	0.005	–	0.0007	–
100 kVp	9.5 (2.7)	6.1–13.5	8.9 (1.4)	6.6–11.8
OBTCM	9.8 (2.5)	6.4–13.6	9.1 (1.6)	6.9–11.4
Difference	0.3	–	0.2	–
p-value	0.25	–	0.73	–
120 kVp	9.1 (2.1)	5.9–12.6	8.1 (1.5)	5.1–9.7
OBTCM	9.5 (2.2)	6.5–12.8	8.6 (1.2)	6.8–10.8
Difference	0.4	–	0.5	–
p-value	0.10	–	0.18	–
140 kVp ^a	8.8 (2.3)	5.6–12.5	7.7 (1.3)	5.6–9.7
OBTCM	9.6 (2.0)	6.1–12.2	7.5 (1.5)	5.2–9.9
Difference	0.8	–	–0.2	–
p-value	0.01	–	0.41	–

Statistically significant ($p < 0.05$) results are marked in bold.^a 135 kVp in Canon.

Discussion

In this experimental phantom study we assessed radiation dose and image quality with and without OBTCM in scanners from three major vendors.

Radiation dose reduction

The GE Revolution CT had the lowest overall radiation dose and the highest dose reduction with OBTCM engaged. The dose reduction across kVps was comparable to those of a previous

Table 6

Size, attenuation and frequency of missed tumours with and without OBTCM across vendors. Three observers; n = 72, no. of observations = 216.

Tumour size	Attenuation (HU)	OBTCM (n)	Non-OBTCM (n)
5 mm	+100	3	9
	-630	11	11
8 mm	+100	1	3
	-630	5	1
12 mm	+100	1	2
	-630	3	3
Total		24	29

study.⁸ Even though the Canon Aquillion Prime is a mid-range scanner, radiation doses were quite low, but the dose reduction with OBTCM was moderate compared to the high-end GE scanner. With the Siemens Somatom Flash scanner, we found that at 80, 120 and 140 kVp both the total dose and the anterior dose were significantly higher with OBTCM engaged compared with non-OBTCM. This finding was surprising and not in line with previous studies.^{1,4,16,26,27} With OBTCM the pitch cannot be altered⁵ and thus, the result may be caused by pitch difference between the standard protocol (pitch 1.2) and the OBTCM protocol (pitch 0.6) as the before mentioned studies used lower pitch settings (between 0.5 and 0.9) for the standard CT protocol. The results suggest that Siemens' OBTCM system may not automatically be advantageous for the patient and the person responsible for CT protocol development should ensure that the total dose is similar to that of non-OBTCM before incorporating it into the CT protocols. Further clinical studies comparing OBTCM and non-OBTCM in different anatomical positions using different pitch settings are needed.

Image quality

GE and Canon CT scanners lower the radiation dose in the anterior segment and noise should increase resultantly. However, we found very little noise differences between OBTCM and non-OBTCM. Siemens has chosen a different strategy with increased tube current in the posterior tube angles to maintain image noise at the same level.²⁸ The images acquired with this scanner were slightly less noisy compared with the other vendors, but none of the vendors had clinically relevant noise differences between scans performed with and without OBTCM, respectively.

All images were acceptable for diagnostic use and we found no statistically significant difference in subjective image quality in any of the scanners; neither with respect to overall image quality nor within individual VGA criteria (data not shown). Furthermore, the radiologists correctly identified most tumours both with and without OBTCM. Small tumours with low attenuation had the highest rate of missed tumours. However, the rate of missed tumours may be explained by the use of 5 mm slices and because the radiologists viewed a large bulk of almost identical images in one or two sessions fatigue was not unlikely to occur and might also explain the results. We found no obvious pattern in missed lesions with regard to OBTCM versus non-OBTCM and thus, the detection rates might differ for the above mentioned reasons.

The poor inter-observer reliability found in this study may partly be explained by differences in experience. The more experienced observer had better intra-observer agreement compared with the other observers even though the kappa value reflected weak agreement. Thus, the poor inter-observer agreement cannot solely be explained by seniority, but also lack of consensus must be considered as an explanation, despite the fact that the three observers work closely together in the same imaging section and solve similar tasks. As the VGA results were in line with the noise

measurements we find that the image quality assessment reflects reality despite poor inter- and intra-observer reliability.

The study has some limitations. The breast phantom was designed to mimic the density and size of female breasts, but they were less flexible and they would fall off if positioned more laterally. In a patient, breast tissue may be outside the OBTCM-range,^{1,29} but the percentage of breast tissue within the range can be increased by wearing a bra.³⁰ Thus, the experimental setup mimics an ideal situation where all of the breast tissue is located within the modulation range. Furthermore, we used a single phantom with average breast size, but a retrospective study found that OBTCM tended to be more effective in high-BMI patients.³ The TLDs were positioned under the breasts, as this was an easily reproducible method. Other positions such as inside the phantom might have affected the measurements, but we do not think it would affect the overall results of the study. Finally, TLDs could have been calibrated instead using an X-ray source such as the CT scanner to replicate the rotational influence of CT as well as matching the energy of the X-ray beam,³¹ however radioactive sources are more stable in output and the national standard.

In conclusion, organ based tube current modulation is capable of anterior and total dose reduction with minimal loss of image quality and tumour visibility in vendors that do not increase posterior dose. However, OBTCM did not function as expected across all vendors and further investigations are required to ensure such software delivers dose reductions to the intended radiosensitive organs.

Ethical review board

Ethical approval was waived in this phantom study according to Danish legislation.

Location

The study was performed at the Department of Radiology at Odense University Hospital, DK-5000 Odense C.

Level of evidence

Experimental phantom study.

Conflict of interest statement

None.

Acknowledgements

We would like to express our gratitude to the radiographers Joakim Dam Hansen and Kolbjørn Donslund Nielsen for their great help gathering data for the study.

This research did not receive any specific grant from funding agencies in the public, commercial, or not-for-profit sectors.

References

- Euler A, Szucs-Farkas Z, Falkowski AL, Kawel-Bohm N, D'Errico L, Kopp S, et al. Organ-based tube current modulation in a clinical context: dose reduction may be largely overestimated in breast tissue. *Eur Radiol* 2016;**26**(8):2656–62.
- Fu W, Sturgeon GM, Agasthya G, Segars WP, Kapadia AJ, Samei E. Breast dose reduction with organ-based, wide-angle tube current modulated CT. *J Med Imaging (Bellingham)* 2017;**4**(3):31208.
- Akai H, Kiryu S, Shibata E, Maeda E, Sato J, Tomizawa N, et al. Reducing CT radiation exposure with organ effective modulation: a retrospective clinical study. *Eur J Radiol* 2016;**85**(9):1569–73.

4. Duan X, Wang J, Christner JA, Leng S, Grant KL, McCollough CH. Dose reduction to anterior surfaces with organ-based tube-current modulation: evaluation of performance in a phantom study. *Am J Roentgenol* 2011;**197**(3):689–95.
5. Lungren MP, Yoshizumi TT, Brady SM, Toncheva G, Anderson-Evans C, Lowry C, et al. Radiation dose estimations to the thorax using organ-based dose modulation. *Am J Roentgenol* 2012;**199**(1):W65–73.
6. Gandhi D, Crotty DJ, Stevens GM, Schmidt TG. Technical note: phantom study to evaluate the dose and image quality effects of a computed tomography organ-based tube current modulation technique. *Med Phys* 2015;**42**(11):6572–8.
7. Matsubara K, Sugai M, Toyoda A, Koshida H, Sakuta K, Takata T, et al. Assessment of an organ-based tube current modulation in thoracic computed tomography. *J Appl Clin Med Phys* 2012;**13**(2):3731.
8. Dixon MT, Loader RJ, Stevens GC, Rowles NP. An evaluation of organ dose modulation on a GE optima CT660-computed tomography scanner. *J Appl Clin Med Phys* 2016;**17**(3):380–91.
9. Kim YK, Sung YM, Choi JH, Kim EY, Kim HS. Reduced radiation exposure of the female breast during low-dose chest CT using organ-based tube current modulation and a bismuth shield: comparison of image quality and radiation dose. *Am J Roentgenol* 2013;**200**(3):537–44.
10. Lambert JW, Gould RG. Evaluation of a net dose-reducing organ-based tube current modulation technique: comparison with standard dose and bismuth-shielded acquisitions. *Am J Roentgenol* 2016;**206**(6):1233–40.
11. AAPM. *AAPM position statement on the use of bismuth shielding for the purpose of dose reduction in CT scanning*. PP 26-B. United States: The American association of Physicists in Medicine; 2017.
12. Becker HC, Augart D, Karpitschka M, Ulzheimer S, Bamberg F, Morhard D, et al. Radiation exposure and image quality of normal computed tomography brain images acquired with automated and organ-based tube current modulation multiband filtering and iterative reconstruction. *Investig Radiol* 2012;**47**(3):202–7.
13. Boos J, Kropil P, Klee D, Heusch P, Schimmoller L, Schaper J, et al. Evaluation of the impact of organ-specific dose reduction on image quality in pediatric chest computed tomography. *Pediatr Radiol* 2014;**44**(9):1065–9.
14. Hoang JK, Yoshizumi TT, Choudhury KR, Nguyen GB, Toncheva G, Gaftan AR, et al. Organ-based dose current modulation and thyroid shields: techniques of radiation dose reduction for neck CT. *Am J Roentgenol* 2012;**198**(5):1132–8.
15. Kim JS, Kwon SM, Kim JM, Yoon SW. New organ-based tube current modulation method to reduce the radiation dose during computed tomography of the head: evaluation of image quality and radiation dose to the eyes in the phantom study. *Radiol Med* 2017;**122**(8):601–8.
16. Wang J, Duan X, Christner JA, Leng S, Grant KL, McCollough CH. Bismuth shielding, organ-based tube current modulation, and global reduction of tube current for dose reduction to the eye at head CT. *Radiology* 2012;**262**(1):191–8.
17. Marsh RM, Silosky M. Characterization and implementation of OSL dosimeters for use in evaluating the efficacy of organ-based tube current modulation for CT scans of the face and orbits. *Med Phys* 2015;**42**(4):1730–8.
18. Erić M, Anderla A, Stefanović D, Drapšin M. Breast volume estimation from systematic series of CT scans using the Cavalieri principle and 3D reconstruction. *Int J Surg* 2014;**12**(9):912–7.
19. Bankier AA, MacMahon H, Goo JM, Rubin GD, Schaefer-Prokop CM, Naidich DP. Recommendations for measuring pulmonary nodules at CT: a statement from the Fleischner Society. *Radiology* 2017;**285**(2):584–600.
20. Månsson LG. Methods for the evaluation of image quality: a review. *Radiat Prot Dosim* 2000;**90**(1–2):89–99.
21. Ludewig E, Richter A, Frame M. Diagnostic imaging – evaluating image quality using visual grading characteristic (VGC) analysis. *Vet Res Commun* 2010;**34**(5):473–9.
22. Hakansson M, Svensson S, Zachrisson S, Svallkvist A, Bath M, Mansson LG. VIEWDEX: an efficient and easy-to-use software for observer performance studies. *Radiat Prot Dosim* 2010;**139**(1–3):42–51.
23. Borjesson S, Hakansson M, Bath M, Kheddache S, Svensson S, Tingberg A, et al. A software tool for increased efficiency in observer performance studies in radiology. *Radiat Prot Dosim* 2005;**114**(1–3):45–52.
24. Kusk MW, Karstoft J, Mussmann BR. CT triage for lung malignancy: coronal multiplanar reformation versus images in three orthogonal planes. *Acta Radiol* 2015;**56**(11):1336–41.
25. McHugh ML. Interrater reliability: the kappa statistic. *Biochem Med (Zagreb)* 2012;**22**(3):276–82.
26. Ketelsen D, Buchgeister M, Fenchel M, Schmidt B, Flohr TG, Syha R, et al. Automated computed tomography dose-saving algorithm to protect radio-sensitive tissues: estimation of radiation exposure and image quality considerations. *Investig Radiol* 2012;**47**(2):148–52.
27. Franck C, Smeets P, Lapeire L, Achten E, Bacher K. Estimating the patient-specific dose to the thyroid and breasts and overall risk in chest CT when using organ-based tube current modulation. *Radiology* 2018;**288**(1):164–9.
28. Yamauchi-Kawaura C, Yamauchi M, Imai K, Ikeda M, Aoyama T. Image quality and age-specific dose estimation in head and chest CT examinations with organ-based tube-current modulation. *Radiat Prot Dosim* 2013;**157**(2):193–205.
29. Taylor S, Litmanovich DE, Shahrzad M, Bankier AA, Gevenois PA, Tack D. Organ-based tube current modulation: are women's breasts positioned in the reduced-dose zone? *Radiology* 2015;**274**(1):260–6.
30. Seidenfuss A, Mayr A, Schmid M, Uder M, Lell MM. Dose reduction of the female breast in chest CT. *Am J Roentgenol* 2014;**202**(5):W447–52.
31. Maia AF, Caldas LVE. A rotational calibration method using thermoluminescent dosimeters for dose determination in computed tomography beams. *Nucl Instrum Methods Phys Res Sect B Beam Interact Mater Atoms* 2008;**266**(1):107–10.